Gonzalez, Y., Nelson, D. D., Shorter, J. H., McManus, J. B., Dyroff, C., Formolo, M., Wang, D. T., Western, C. M., & Ono, S. (2019). Precise Measurements of $^{12}CH_2D_2$ by Tunable Infrared Laser Direct Absorption Spectroscopy. *Analytical Chemistry*, *91*, 14967-14974. [23]. https://doi.org/10.1021/acs.analchem.9b03412

Precise measurements of $^{12}CH_2D_2$ by tunable infrared laser direct absorption spectroscopy

Yenny Gonzalez[†¥], David D. Nelson[§], Joanne H. Shorter[§], Barry J. McManus[§], Christoph Dyroff[§], Michael Formolo[‡], David T. Wang[‡], Colin M. Western[ϑ], Shuhei Ono[*,†].

[†] Department of Earth, Atmospheric and Planetary Sciences, Massachusetts Institute of Technology, Cambridge, MA 02139, USA, [*]sono@mit.edu.

[¥] Now at Department of Earth and Planetary Sciences, School of Engineering and Applied Sciences, Harvard University, Cambridge, MA 02138, USA.

[§] Center for Atmospheric and Environmental Chemistry, Aerodyne Research, Inc., Billerica, MA 01821, USA

[‡] ExxonMobil Upstream Research Company, 22777 Springwoods Village Parkway, Spring, Texas 77389, USA.

[ϑ] School of Chemistry, University of Bristol, Cantock's Close, Bristol BS8 1TS, UK.

KEYWORDS spectroscopy, methane, isotopologues

ABSTRACT. We present precise measurements of doubly-deuterated methane ($^{12}CH_2D_2$) in natural methane samples using tunable infrared laser direct absorption spectroscopy (TILDAS). Using a 413 m optical path length astigmatic Herriott cell and two quantum cascade lasers (QCLs) scanning the spectral regions of 1090.46 ± 0.1 cm^{-1} and 1200.23 ± 0.1 cm^{-1}, the instrument simultaneously measures the five main isotopologues of methane. The ratios $^{13}CH_3D/^{12}CH_4$ and $^{12}CH_2D_2/^{12}CH_4$ are measured at 0.01‰ and 0.5‰ (1σ) instrumental precision, respectively. The instrumental accuracy was assessed by measuring a series of methane gases with a range of $\delta^{13}C$ and δD values but with the abundances of all isotopologues driven to thermal equilibrium at 250 °C. The estimated accuracy of $\Delta^{12}CH_2D_2$ is 1‰ (1σ) based on the results of the heated methane samples. This new TILDAS instrument provides a simple and rapid technique to explore the sources of methane in the environment.

Understanding the origins of methane is crucial for predicting the methane atmospheric budget,[1] locating natural gas deposits for energy production,[2] and for exploring the potential for extraterrestrial life.[3] The origins of methane have traditionally been studied based on the analysis of its carbon ($^{13}C/^{12}C$) and hydrogen (D/H) stable isotope ratios.[4] These ratios reflect both the origin of carbon and hydrogen and the isotope fractionation during its formation. In addition to traditional bulk isotope ratios, abundances of methane isotopologues (molecules with different isotope configurations) that contain more than one rare isotope, $^{13}CH_3D$ and $^{12}CH_2D_2$, have recently been explored as novel proxies.[5,6,7] Because isotopologue distribution is expected to be a function of temperature (under equilibrium condition), the abundance of these multiply-substituted "clumped" isotopologues may carry infor-

mation regarding the generation temperature of methane.[5,6] In order for the clumped methane thermometer to provide useful information, a measurement precision better than 0.3‰ is required for the ratio $^{13}CH_3D/^{12}CH_4$ (corresponding to ± 10 °C at 35 °C).[5,6] For the ratio $^{12}CH_2D_2/^{12}CH_4$ the equivalent precision required is 1.4‰ at the same temperature range. This poses an analytical challenge due to the low abundances of these isotopologues (~7 ppm and 0.14 ppm fractional abundance for $^{13}CH_3D$ and $^{12}CH_2D_2$, respectively) and the wide range of deuterium abundances (D/H ≃ 90 to 150 ppm) over which the measurement must remain linear. Due to isobaric interferences (i.e., $^{13}CH_4$ and $^{12}CH_3D$ on mass-17), isotope ratios of methane had been measured by combustion to CO_2 and H_2O followed by reduction of H_2O to H_2, and measurements of CO_2^+ and H_2^+ ions produced by an electron impact ion source in an isotope-ratio mass spectrometer.[8] The conventional technique just described destroys all information about the abundances of individual isotopologues.

Recent advances in high mass resolution-isotope ratio-mass spectroscopy[5,9] and mid-infrared laser spectroscopy[6] instruments have enabled precise and accurate measurements of methane stable isotopologues at natural-abundance levels. Stolper et al. (2014)[5] measured combined molecular ions at mass-18 ($^{13}CH_3D^+$ and $^{12}CH_2D_2^+$) and corrected for an adduct ion ($^{13}CH_5^+$). A mass resolution from 16,000 to 25,000 was used to resolve two ions ($^{12}CH_3D^+$ and $^{13}CH_4^+$) on mass-17.[5] A later study by Young et al. (2017)[9] demonstrated precise and accurate measurements by resolving $^{13}CH_3D^+$ and $^{12}CH_2D_2^+$ ions at a mass-resolving power of >40,000. Due to its low fractional abundance, the $^{12}CH_2D_2$ beam intensity is low (200 to 300 counts per second). This instrument achieved ~0.5‰ precision (1-SE) for $^{12}CH_2D_2$ after ~ 20 hours of measurement time per sample. Mid and near-infrared spectroscopy offers an alternative means for high precision measurements of isotopologues of small molecules.[10,11] Ono et al.[6] demonstrated the precise and accurate measurement of $^{13}CH_3D$ using a tunable infrared laser direct absorption spectrometry (TILDAS) instrument in the mid-infrared (~8 μm wavelength), corresponding to C-D and C-H fundamental bending vibration modes. A precision of ± 0.2‰ was obtained for the measurements of $^{13}CH_3D$, by combining the narrow line width (<50 MHz) of quantum cascade lasers (QCLs) and long effective pathlength (76 m) achieved by an astigmatic Herriott direct absorption cell.[12]

Studies of $^{13}CH_3D$ (and combined $^{13}CH_3D$ and $^{12}CH_2D_2$) demonstrated that apparent temperatures derived from clumped isotopologue abundances fall within ranges of geologically-occurring temperatures. These temperatures are thought to be compatible with the generation of methane, in particular, for thermogenic methane from hydrocarbon-producing wells and hydrothermal vents.[5,13] Biogenic methane samples from surface environments (e.g., ruminants, swamps and lakes), however, often exhibit strong kinetic signals with apparent isotopologue temperatures much higher than the actual temperature of generation. Although kinetic signals can be discerned by comparing the D/H ratio of methane and associated water,[13,14] water samples may not always be available. Here, measurements of the next rarest isotopologue, $^{12}CH_2D_2$, are particularly useful since data on its abundance can distinguish kinetically-influenced versus equilibrated isotopologue signals based on no other data than the relative abundance of methane isotopologues.[9]

We present the first direct measurements of $^{12}CH_2D_2$ at natural abundance using an optical spectrometer. Using a 413 m optical path length provided by an astigmatic Herriot cell and two QCLs to scan two spectral regions in the mid-infrared, the TILDAS instrument simultaneously measures the relative abundance of five isotopologues of methane ($^{12}CH_4$, $^{13}CH_4$, $^{12}CH_3D$, $^{13}CH_3D$, and $^{12}CH_2D_2$). An inlet manifold was constructed to allow repeated measurements of the sample methane. We report the precision and accuracy of the instrument evaluated by the measurements of a series of synthetic and natural methane samples with a range of isotopic compositions.

PRINCIPLE OF METHANE CLUMPED ISOTOPE THERMOMETER

In this paper, we report isotopologue abundance in a conventional delta notation. For example,

$$\delta^{12}\mathrm{CH_2D_2} = \frac{([^{12}\mathrm{CH_2D_2}]/[^{12}\mathrm{CH_4}])_{sample}}{([^{12}\mathrm{CH_2D_2}]/[^{12}\mathrm{CH_4}])_{reference}} - 1 \qquad (1)$$

For natural isotopologue abundance methane, conventional $\delta^{13}C$ and δD values equal $\delta^{13}CH_4$ and $\delta^{12}CH_3D$, respectively, within the level of uncertainty. The values for $\delta^{13}C$ and δD were normalized against Pee Dee Belemnite (PDB) and Standard Mean Oceanic Water (SMOW) based on the $\delta^{13}C$ and δD values of -29.0‰ and -138‰ for NGS-1, and -72.8‰ and -176‰ for NGS-3, respectively.[13,15]

Methane isotopologue geothermometry is based on the following two reactions:

$$^{13}\mathrm{CH_4} + {}^{12}\mathrm{CH_3D} \rightleftharpoons {}^{12}\mathrm{CH_4} + {}^{13}\mathrm{CH_3D} \qquad (2)$$

$$2\,{}^{12}\mathrm{CH_3D} \rightleftharpoons {}^{12}\mathrm{CH_4} + {}^{12}\mathrm{CH_2D_2} \qquad (3)$$

The equilibrium constants (*K1 and K2*) for these reactions are both primarily functions of temperature. At very high temperatures (> 1000 K) all isotopes distribute stochastically among all isotopologues and *K1* (from the reaction in eq. 2) approaches unity and *K2* (from eq. 3) approaches 3/8. At lower temperatures, isotopologues with two heavy isotopes are favored and the *K* values deviate from the limiting values. We use $\Delta^{13}CH_3D$ and $\Delta^{12}CH_2D_2$ values to represent the deviations of the abundance of $^{13}CH_3D$ and $^{12}CH_2D_2$ from that expected from high temperature (stochastic) distributions:

$$\Delta^{13}\mathrm{CH_3D} = \ln\left(\frac{[^{13}\mathrm{CH_3D}][^{12}\mathrm{CH_4}]}{[^{13}\mathrm{CH_4}][^{12}\mathrm{CH_3D}]}\right) = \ln\left(\frac{[^{13}\mathrm{CH_3D}]}{[^{12}\mathrm{CH_3D}]}\right) - \ln\left(\frac{[^{13}\mathrm{CH_4}]}{[^{12}\mathrm{CH_4}]}\right) \quad \text{, and (4)}$$

$$\Delta^{12}\mathrm{CH_2D_2} = \ln\left(\frac{[^{12}\mathrm{CH_2D_2}][^{12}\mathrm{CH_4}]}{[^{12}\mathrm{CH_3D}][^{12}\mathrm{CH_3D}]}\right) = \ln\left(\frac{[^{12}\mathrm{CH_2D_2}]}{[^{12}\mathrm{CH_3D}]}\right) - 2\ln\left(\frac{[^{12}\mathrm{CH_3D}]}{[^{12}\mathrm{CH_4}]}\right) \text{ . (5)}$$

The temperature dependence of the isotopologue exchange reactions can be estimated by *ab initio* molecular simulations.[5,6,16] We used the temperature dependence of equilibrium constants reported in Young et al. (2017)[9].

EXPERIMENTAL SECTION

Spectral simulation of $^{12}CH_2D_2$. In order to select a possible spectral region for the measurement of $^{12}CH_2D_2$ using TILDAS instrument, we made a spectroscopic model of $^{12}CH_2D_2$. The model was used to generate a line list for $^{12}CH_2D_2$ because one was not available in the HITRAN database.[17] We used the open source program PGOPHER[18] and the work of Ulenikov et al. (1994)[19] to determine the line positions and strengths for ro-vibrational absorption lines of $^{12}CH_2D_2$. We focused on the spectral region between 900 and 1500 cm^{-1}, corresponding to the fundamental C-D and C-H bending vibrational modes, ν_3, ν_4, ν_7 and ν_9. Our choice was based on our experience from the previous TILDAS for $^{13}CH_3D$ at 1168 cm^{-1}.[6] Other candidate regions to possibly explore in the future are the 2134.75 cm^{-1} (ν_2) and 2217.65 cm^{-1} (ν_8) bands which correspond to the C-D stretching vibrations. Due to the large D/H isotope shifts, less interferences are expected from more abundant isotopologues ($^{12}CH_4$ and $^{13}CH_4$) compared to C-D bending regions.[20] For the region 900 and 1500 cm^{-1}, Ulenikov et al. (1994)[19] found significant Coriolis interactions between the upper states (their Table VII), sufficient to affect intensities and therefore requiring a model including several states is required. As their model was difficult to reproduce exactly, we instead used a simplified model with fewer Coriolis interaction terms, including only the leading Coriolis interaction terms (proportional to J_a, J_b or J_c).[19] The ground state and infrared inactive $\nu_5 = 1$ constants were used directly from Ulenikov et al.[19] (23 parameters), but constants for $\nu_3 = 1$, $\nu_4 = 1$, $\nu_7 = 1$ and $\nu_9 = 1$ were derived by refitting the energy levels to those published by Ulenikov et al. (1994,Tables III and IV).[19] The nine leading Coriolis interaction terms were set to the values given by Ulenikov et al[19] derived from values for CH_4 and all others Coriolis terms fixed at zero. This approach produced a good fit (average error 0.0016 cm^{-1} for $J' \leq 15$ compared with 0.00015 cm^{-1} from the previous work) but with fewer parameters (88 rather than 93 total rotational, centrifugal and interaction parameters used by Ulenikov et al[19]) and is sufficient for our purposes. The details of the fit, including the constants used and a table of observed – calculated values are given in Tables S-1, S-2 and S-3 of the supporting information.

We obtained relative line strengths within each band system (ν_3,ν_4,ν_7 and ν_9) using PGOPHER. However, it is necessary to include the effect of the vibrational transitional moments to properly simulate absolute line strengths, especially given the significant Coriolis mixing between states. We adjusted the transition moments to reproduce the measured spectra reported in Ulenikov et al. (1994, Figures 1-3; experimental conditions: 3.2 m of path length at 0.11 Torr and at room temperature, assumed 296 K, linewidth 0.003 – 0.0047 cm^{-1} depending on frequency).[19] *See* Figure S-1 of the Supporting Information. This process gives a reasonable estimate of the absolute intensities, though with limited accuracy at this stage.

Line positions and strengths of $^{12}CH_2D_2$ (calculated with PGOPHER) and four other methane isotopologues ($^{12}CH_4$, $^{13}CH_4$, $^{12}CH_3D$ and $^{13}CH_3D$ from HITRAN database) in the region between 950 and 1500 cm^{-1} are shown in Figure 1. Using this line list, we simulated the molecular spectrum applicable for our TILDAS instrument (413 m path length and cell pressure at 5 Torr). After careful and detailed examination, we chose the spectral region around

1090 cm^{-1} to measure $^{12}CH_2D_2$ with TILDAS. A large number of interfering absorptions of more abundant isotopologues (weak lines of $^{12}CH_4$ in particular) excluded most of the regions above ca. 1150 cm^{-1} for the measurements of $^{12}CH_2D_2$. Pressure broadening coefficients (self-broadening) of the selected $^{12}CH_2D_2$ lines were derived by fitting TILDAS spectrum (Table 1).

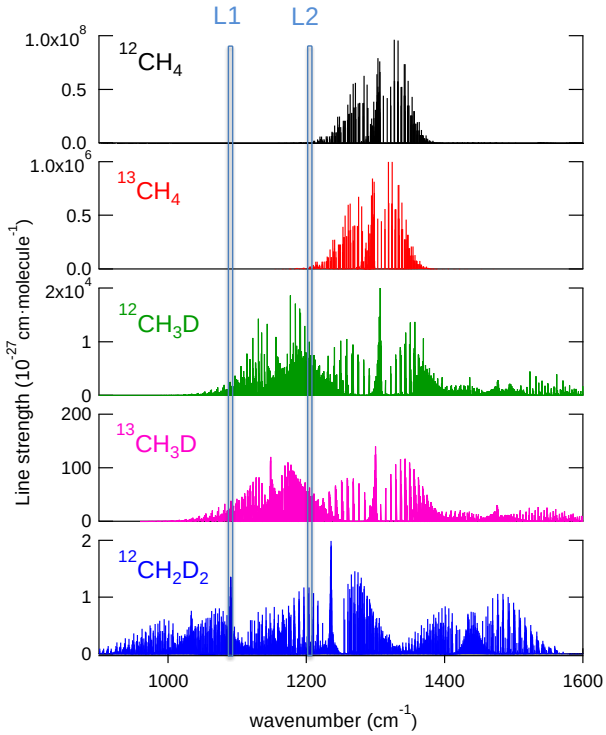

Figure 1. Line positions and strength for the five major isotopologues of methane. Data for the $^{12}CH_2D_2$ spectrum are from this study, and those for $^{12}CH_4$, $^{13}CH_4$, $^{12}CH_3D$ and $^{13}CH_3D$ isotopologues are from HITRAN 16. Two spectral regions selected for TILDAS measurements (L1 and L2) are also shown. Line strengths are normalized by natural isotopologue abundance following the convention of the HITRAN database. We assumed isotopologue abundance of $^{12}CH_2D_2$ of $1.44 \cdot 10^{-7}$ with respect $^{12}CH_4$.

Specifications of $^{12}D_2$-TILDAS. We used a TILDAS instrument (Aerodyne Research Inc., Billerica MA) to measure $^{12}CH_2D_2$. The high spectral resolution is achieved by the use of quantum cascade lasers (QCLs, Alpes Lasers, Switzerland). These lasers provide high optical power (10 to 100 mW), narrow band (<30 MHz) and single mode operation.[21] In our project, we used two QCLs to scan absorption lines of the 5 main isotopologues of methane. This allows us to obtain simultaneous measurements of four isotopologue ratios of methane ($\delta^{13}C$, δD, $\Delta^{13}CH_3D$ and $\Delta^{12}CH_2D_2$). Peltier elements control the temperature of the sealed laser housings at -11.7 ˚C and -21.4 ˚C for laser 1 (L1) and laser 2 (L2), respectively. The supply currents to the QCLs are ramped at a rate of 1.4 kHz to scan the laser frequency for 450 channels in L1 and 350 in L2, with extra 100 channels to measure the laser shut off (zero-light levels). The laser frequency tuning rates are measured by a germanium etalon and fitted with a cubic spline function. We used an astigmatic multipass absorption cell with an effective path length of 413 m (~2.8 L of

volume, including dead volume). Temperature and pressure are monitored inside the cell with a 30 kΩ thermistor and a capacitance manometer (40 Torr full scale, MKS, Andover, MA). The number density of each isotopologue is derived at a rate of 1 Hz by a least squares spectral fit assuming the Voigt line profile at the pressure and temperature measured inside the cell.

Description of measured spectral regions. The line positions and strengths, lower state of energy and temperature dependence of the target lines are shown in Table 1. The additional lines included in the spectral fit are shown in Table S-4 of Supporting Information.

One QCL (L1) scans the spectral interval 1090.46 ± 0.1 cm^{-1}. Here, we measure a $^{12}CH_2D_2$ doublet at 1090.3900 and 1090.3937 cm^{-1} (Q-branch of ν_7), a $^{12}CH_4$ line at 1090.471 cm^{-1}, and a $^{12}CH_3D$ line at 1090.509 cm^{-1} (Figure 2). The $^{12}CH_3D$ line is not included in the HITRAN-2016[17] but identified by the measurements of a pure $^{12}CH_3D$ sample (*see* Section 1 of the Supporting Information). For a natural abundance methane sample at 5 Torr (413 m pathlength), the fraction of absorption of these three lines are 0.15% for $^{12}CH_2D_2$, and 1% for $^{12}CH_4$ and $^{12}CH_3D$, respectively (Figure 2).

A second QCL (L2) is tuned to measure $^{12}CH_4$, $^{13}CH_4$, $^{12}CH_3D$ and $^{13}CH_3D$ lines simultaneously at 1200.23 ± 0.07 cm^{-1}. The target lines are measured at the following positions: $^{12}CH_4$ at 1200.1994 cm^{-1}, $^{13}CH_4$ at 1200.2182 cm^{-1}, $^{12}CH_3D$ at 1200.2416 cm^{-1} and $^{13}CH_3D$ at 1200.2627 cm^{-1} (Table 1). The fraction of absorption of these four lines for natural abundance methane at 5 Torr are 47% for $^{12}CH_4$, 10% $^{13}CH_4$, 4.5% for $^{12}CH_3D$+$^{12}CH_4$ (~60% is due to $^{12}CH_4$) and 7% for $^{13}CH_3D$, respectively.

Table 1. Line position (LP), strength (LS), lower state of energy (E"), temperature dependence (dδ/dT) and self-broadening coefficients (γ_{self}) of the target lines.

Isotopologue	LP (cm^{-1})	LS (cm/molecule)	*E"* (cm^{-1})	dδ/dT (‰/10 mK)	γ_{self} (cm^{-1}/atm)
		Target lines			
$^{12}CH_4$	1200.19935	$4.692 \cdot 10^{-25}$	2493.131	0.41	0.067
$^{13}CH_4$	1200.21820	$7.780 \cdot 10^{-26}$	2045.419	0.34	0.063
$^{12}CH_3D$	1200.24160	$1.444 \cdot 10^{-26}$	976.363	0.16	0.062
($^{12}CH_4$)*	1200.24150	$2.110 \cdot 10^{-26}$	2796.740	0.46	0.065
$^{13}CH_3D$	1200.26267	$5.678 \cdot 10^{-26}$	222.410	0.04	0.082
$^{12}CH_2D_2$	1090.39000	$1.068 \cdot 10^{-27}$	175.928	0.03	0.064
	1090.39370	$6.790 \cdot 10^{-28}$	140.640	0.02	0.064

*This $^{12}CH_4$ line overlaps with $^{12}CH_3D$.

We experimentally confirmed our spectral simulation by measuring a series of isotopologue labeled methane samples, including CH_2D_2 (98% atom purity), $^{12}CH_4$ (99.95% ^{12}C), $^{13}CH_4$ (99% ^{13}C), and CH_3D (98% D) (all from Cambridge Isotope Laboratory, Andover, MA) and D-depleted CH_4 (3 ppm D) that was synthesized in the laboratory.[6] While the data largely corroborated the line lists in HITRAN 16[17] for the four major isotopologues, we identified an additional $^{12}CH_3D$ line at 1090.5 cm^{-1} that we then included in our line list (*see* Table S-4 of the Supporting Information).

We evaluated the effect on the isotopologue ratios of a trace amount of water in the sample. By flowing water saturated air through the cell, we measured three weak water lines in the L1 spectral region, one of which overlapped with $^{12}CH_2D_2$. These lines were included in the fit. The water content of the sample must remain below 250 ppm for $\Delta^{12}CH_2D_2$ precision better than 1‰ (*see* Section 2 of the Supporting Information).

The measured temperature of the TILDAS absorption cell is stable at ±10 mK for a measurement cycle. The temperature dependence of the selected lines was estimated from their lower-state energy and listed in Table 1. Temperature dependence for the isotopologue ratios are as much as 0.4‰/10mK for $\delta^{12}CH_2D_2$ but 0.15‰/10mK for $\Delta^{12}CH_2D_2$ values, because the temperature dependence cancels out. Similarly, the temperature dependence for the $\delta^{12}CH_3D$ (1200.2420 cm^{-1}) that is measured by the overlapping $^{12}CH_3D$ and $^{12}CH_4$ lines is ~0.16‰/10 mK. This relatively minor temperature dependence is because of the similar temperature dependence for the $^{12}CH_4$ lines at 1200.1994cm^{-1} and 1200.24163cm^{-1} (0.46 versus 0.41‰/10 mK, respectively).

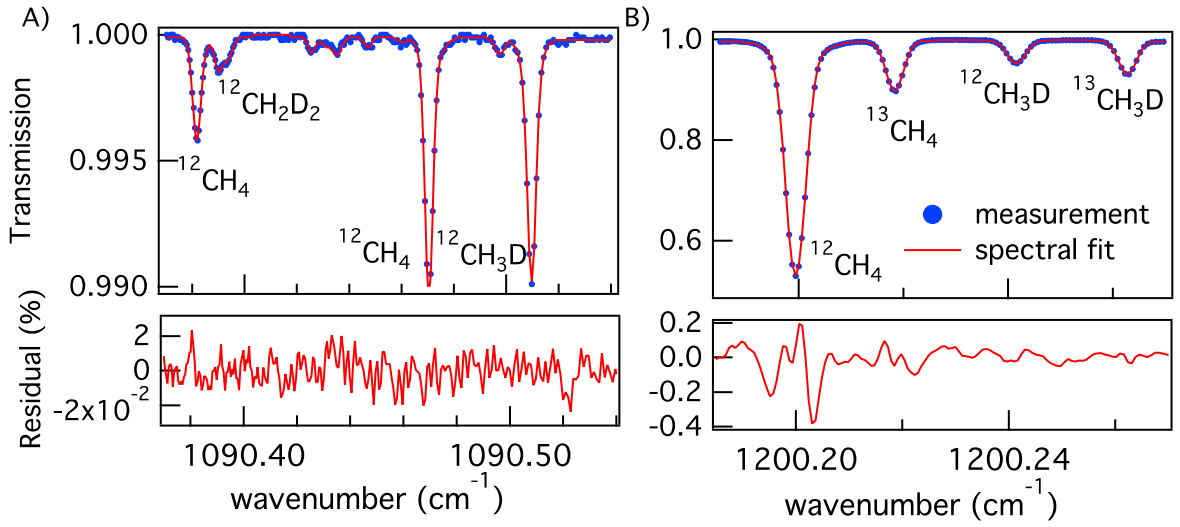

Figure 2. TILDAS spectra and fit residual for methane. Left panel (A) shows Laser 1 (targeting $^{12}CH_2D_2$) and right (B) is for Laser 2 ($^{12}CH_4$, $^{13}CH_4$, $^{12}CH_3D$ and $^{13}CH_3D$). The absorption cell was filled with 5 Torr of methane (laboratory reference gas, AS1) and pathlength 413 m. In top plots, measurements are blue dots and the spectral fit as a red line. The lower plots represent the residual (relative difference between measured and fit spectrum in %).

Gas inlet system. A gas inlet system was built to interface with the D_2-TILDAS. The inlet consists of 15 pneumatically operated bellows-sealed valves (SS-8BK-VCR-1C, Swagelok, Billerica, MA), 4 pressure transducers (Type 722B, MKS, Andover, MA), an adjustable bellows volume (Metal Flex, Newport, VT) controlled with an electronic linear actuator, 2 scroll pumps (IDP-15, Agilent, Lexington, MA), a turbo-molecular pump (TwisTorr 84 FS, Agilent, Lexington, MA) and convection and ion gauges (JLC275 and JLC351, Kurt J. Lesker, Jefferson Hills, PA). Most of the gas manifold was built with ½ inch stainless steel tubing with either VCR or ConFlat fittings. These components are monitored or controlled with a data acquisition system (USB-6343, National Instruments,

Woburn, MA) and LabVIEW software (National Instruments, Woburn, MA). S*ee* Figure S-5 of the Supporting Information for a schematic of the inlet system.

To achieve high precision isotopologue analysis by TILDAS, our inlet system is designed to introduce sample or reference methane gas at a constant pressure (*see* Figure S-6 of the Supporting Information for sample pressure dependence). An adjustable bellows volume (18 to 111 ml of internal volume) is used to control the pressure of sample in the TILDAS absorption cell to within ± 0.1 Torr. Reference CH_4, N_2 and He gases are introduced from fixed volumes (150 ml) via flow restrictors (IC-DM4-4-SS, Swagelok, Billerica, MA). The amount of gas was controlled by the flow rate and the pressure monitored with capacitance manometers. The U-trap is filled with silica gel, and is used to collect sample methane by freezing on the silica gel when the U-trap is immersed in liquid nitrogen. Resistive Ni-Cr wire is used to heat the U-trap to thaw methane at 80 °C, and introduced to the TILDAS absorption cell.

RESULTS

Allan-Werle variance and instrumental precision. We evaluated the precision of the instrument by monitoring a methane sample (20 mL STP) sealed in the cell for 2 h. Allan-Werle variance analysis showed 1-second Allan deviations of 0.05, 0.24, 0.07 and 2.32‰ for $\delta^{13}C$, δD, $\delta^{13}CH_3D$ and $\delta^{12}CH_2D_2$, respectively (Figure 3). Ultimate precisions are 0.01, 0.06, 0.01 and 0.26‰ for $\delta^{13}C$, δD, $\delta^{13}CH_3D$ and $\delta^{12}CH_2D_2$, respectively, with 150 second averages. Thus, we used 150 seconds to measure the four isotopologue ratios. Instrumental drift becomes significant after 600 s averaging time.

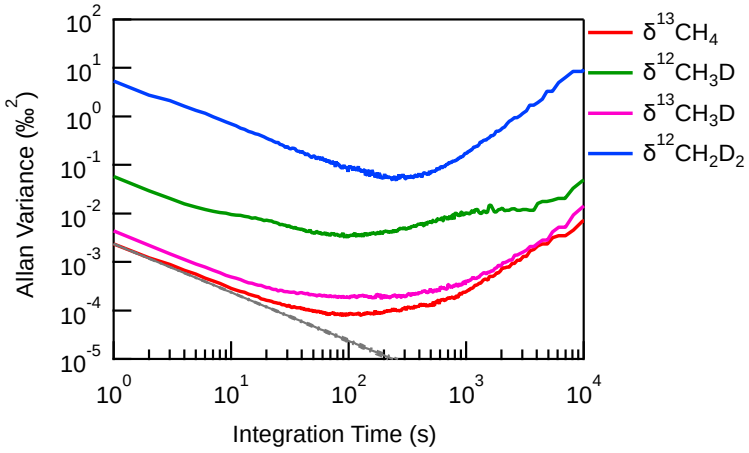

Figure 3. Allan variance analysis of the isotopologues ratios measured in the D_2-TILDAS. Results from a 5 Torr pure methane gas sample.

Measurement cycle. Methane samples are measured by alternately introducing reference and sample methane into TILDAS, equivalent to a dual inlet method for isotope ratio-mass spectrometry. Our inlet system allows multiple measurements of sample methane by freeze-thaw cycles. The measurement cycle was set up as follows. We first freeze sample methane in a U-trap (filled with silica gel) by immersing in liquid nitrogen (LN). The final volume of the sample CH_4 can be adjusted with the bellows volume. Then, the spectral baseline is measured by filling the absorption cell with 7.5 Torr N_2 (ca. 50% higher than CH_4 pressure to compensate for the difference of refractive index). After measuring the baseline, the cell is evacuated using a scroll pump followed by a turbomolecular pump to below a few mTorr as measured by a capacitance manometer attached to the absorption cell. In the evacuated cell, the reference CH_4 is injected at a pressure of 5 ± 0.1 (1-σ) Torr (~20 mL STP) and the isotopologue abundance is measured for 150 seconds. The cell is flushed with He and evacuated to remove the reference gas. Then, the sample is released by heating the U-trap at 80°C and expanded into the cell, where it is measured for 150 seconds at 5 Torr (*see* Figure S-7 of the Supporting Information). After the measurement, the cell containing the methane sample is filled with helium at a total pressure of 10 Torr, and pumped to 1 Torr through the U-trap immersed in LN to freeze methane in the U-trap. Helium does not absorb in the silica gel and is pumped away. This process is repeated 5 times for quantitative (better than 99.99%) recovery of the sample. It was found that the repeated pumping and helium addition is more efficient than pumping down in a single step. One measurement cycle of baseline, sample, and reference measurements takes ca. 26 min, including the 14 min of sample recovery. The measurement cycles are repeated 8 times per sample, providing 8 measurements for the ratios of isotopologue ratios between sample and reference methane.

The overall precision, evaluated from standard deviations of 8 measurement cycles, are 0.02, 0.15, 0.2 and 0.5‰ for $\delta^{13}C$ and δD, $\Delta^{13}CH_3D$ and $\Delta^{12}CH_2D_2$, respectively. These precisions are similar to our previous TILDAS instrument for $^{13}CH_3D$ [6] (*see* Table S-5 of the Supporting Information).

Each time the sample is reintroduced into the cell, the total cell pressure increased by 5 mTorr, indicating that a trace amount of air or helium carrier gas (~20 μL STP) was added to the sample. This increase of matrix gas is due to the limited efficiency of removing the carrier helium gas during the recycling or small leak of air in the vacuum manifold. Methane is efficiently recycled such that its number density, determined from the TILDAS signal for $^{12}CH_4$ line, decreased by less than 500 ppm (0.005‰) per measurement cycle. The additional gas (likely dominantly air) during the recycle run was translated into a reduction of 0.05% of methane mixing ratios after 8 measurement cycles. We did not observe drift in isotopologue ratios during 8 cycles recycling beyond measurement error.

Heated methane calibration. Due to the lack of standard reference materials for methane isotopologues, $\Delta^{13}CH_3D$ and $\Delta^{12}CH_2D_2$ values were calibrated by measuring methane samples that were thermally equilibrated at 250°C using a conventional flame-seal tube technique.[6,13] We created three methane isotopologue mixtures by spiking reference gas (a commercially-sourced methane bottle at natural abundance) with $^{12}CH_3D$ (AL1-D3, δD of

244‰ SMOW), D-depleted CH_4 (AS1-DY, δD of -406‰ SMOW) or ^{13}C-depleted CH_4 (AL1-CD, $\delta^{13}C$ of -82‰ PDB) to cover a range of δD and $\delta^{13}C$ values expected for natural methane samples (Table 2). Aliquots of these isotopologue mixtures and our laboratory reference gases (AL1, AS1, AS2) were frozen in Pyrex tubes containing silica gel and platinum catalyst (Platinum on alumina, Sigma-Aldrich) at -196 °C. These tubes were flame-sealed and heated in an oven at 250 °C for two weeks.

The expected $\Delta^{13}CH_3D$ and $\Delta^{12}CH_2D_2$ values at 250 °C are 2.03‰ and 4.31‰, respectively, and these are not a function of $\delta^{13}C$ or δD values of heated methane. The offset from the expected value was used to derive $\Delta^{13}CH_3D$ and $\Delta^{12}CH_2D_2$ values of laboratory reference gases (AL1 and AS2, Table 2). We found that the isotopologue mixtures yielded measured $\Delta^{13}CH_3D$ and $\Delta^{12}CH_2D_2$ values that are correlated with δD and $\delta^{13}C$ values; ideally this correlation should be zero. The non-linearity is due to insufficient accuracy of our spectral fitting, in particular, the Voigt profile of the near-by strong absorption lines.[6] For example, the $\delta^{12}CH_2D_2$ scale would be contracted (e.g., 100‰ can be measured as 98‰) when the tailing of a near-by line is overestimated due to an estimated negative baseline for the $^{12}CH_2D_2$ (*see* Section 3 of the Supporting Information). We corrected for this effect by adding (or subtracting) a constant to the number density from $^{12}CH_2D_2$. The baseline correction yielded a calculated scale contraction of 0.0009 and 0.028 for in $\delta^{13}CH_3D$ and $\delta^{12}CH_2D_2$, respectively. The scale non-linearity limits the overall accuracy when the sample and reference have very different δD values (e.g., effect is 2.8‰ when $\delta^{12}CH_2D_2$ value of sample is -100‰ with respect to reference). The non-linearity effect is regularly monitored by measuring heated methane samples.

Mixing experiment. We evaluated the linearity of the instrument in $\Delta^{13}CH_3D$ - $\Delta^{2}CH_2D_2$ space by mixing different samples of gas and comparing the measurements of the mixtures to the theoretical mixing curves. We set up three different experiments in which our initial sample was sequentially mixed (from 0 to 100% mole fraction) with our reference gas AS1. Figure 4 shows results of two mixing experiments with initial samples of: A) microbial methane (produced from enriched methanogenic culture using electrodes at ambient temperature) and B) carbon-depleted methane (AL1-CD, Table 2). These samples were sequentially mixed with our reference gas (AS1, likely natural gas that is thermogenic in origin) and measured for isotopologue compositions. The mixing experiments reproduced the theoretical mixing curves between the two end members for $\Delta^{13}CH_3D$ and $\Delta^{12}CH_2D_2$ space, demonstrating the accuracy of the TILDAS instrument (Figure 4).

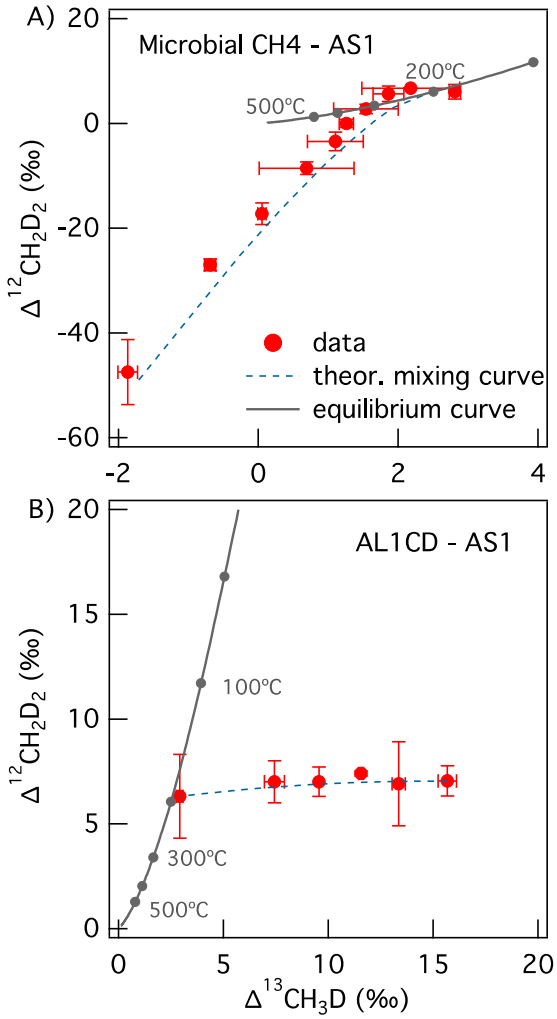

Figure 4. Two mixing experiments: A) First end member: microbial methane, B) First end member: carbon depleted methane (AL1-CD, synthesized in the laboratory). The second end member is our reference gas AS1. The theoretical mixing curves between the end members are shown with blue dashed lines, measurements are in solid circles and the theoretical temperature equilibrium curve is in solid line. The error bars are expressed as average ± 2σ.

Measurement of natural samples. A series of natural methane samples were measured for their $\Delta^{13}CH_3D$ and $\Delta^{12}CH_2D_2$ values (Table 2, Figure 5). These samples include two natural samples (NS1 and NS2) sampled from oil & gas production facilities, one of a microbial methane (EM1) from laboratory methanogenic culture, and two samples from steam vents in the Nisyros Island of Greece. Descriptions of the natural samples are as follows: NS1 is an oil-associated thermogenic gas of early oil window maturity taken from a separator facility on an offshore oil platform and NS2 is a biogenic gas taken from a well casing annulus on an offshore oil platform.

These samples were purified by using cryogenic distillation followed by preparative gas chromatography to remove other gases, including, water, nitrogen, carbon dioxide or larger hydrocarbon molecules that could interfere during the TILDAS analyses[13] (*see* Section 4 of the Supporting Information). Figure 5 and Table 2 list the measured

isotopologue ratios and corresponding apparent equilibrium temperatures based on $\Delta^{13}CH_3D$ and $\Delta^{12}CH_2D_2$ thermometry. Figure 5 also includes results from commercially-purchased pure methane gas tanks (AS1, AS2 and US-1). In addition, these samples were also measured for $\delta^{13}C$, δD and $\Delta^{13}CH_3D$ values using our previous TILDAS as reported in Ono et al., 2014[6] (*see* results in Section 5 of the Supporting Information).

The reference gases AL1, AS2 and US-1 yielded $^{13}CH_3D$ based temperatures (T_{13D}) from 214 to 228°C (Table 2). Their $^{12}CH_2D_2$ based temperatures (T_{12D2}) are largely consistent with T_{13D} within the analytical uncertainty, indicating these gases (likely thermogenic natural gas) are equilibrated or generated via near-equilibrium process at the temperature range 200 to 250°C. Two steam vent samples (SV1 and SV2) also yielded near-equilibrium values for $^{13}CH_3D$ and $^{12}CH_2D_2$, but at much higher temperatures of 400 to 447 °C and above 769°C for T_{13D} and T_{12D2} respectively, compared to the reference gas samples (Figure 4). The discrepancy between T_{13D} and T_{12D2} might reflect their different rates of isotopologue exchange. The $\delta^{13}C$, δD and $\Delta^{13}CH_3D$ values are consistent with previously reported value obtained by isotope ratio-mass spectrometry from the same area.[23,24]

The two natural gas samples, NS1 and NS2 yielded $\Delta^{13}CH_3D$ values for 1.85‰ and 4.47‰, respectively. These values correspond to apparent temperatures from 74°C to 269°C, respectively. These two samples plot slightly away from the equilibrium line (Figure 5), suggesting either mixing of methane with different isotope compositions or kinetic signals from recently generated microbial methane.

Microbial methane (EM1) was produced by a methanogenic community enriched from mud and organic debris collected in a rain-gutter drain that was incubated in medium containing acetate and electrodes. 16S RNA analysis showed predominance of hydrogenotrophic methanogens (mostly *Methanomicrobiales* and *Methanobacterium* sp.). This methane carried negative values of $\Delta^{13}CH_3D$ and $\Delta^{12}CH_2D_2$ of -1.91‰ and -47.5‰, respectively, and therefore correspond to no real apparent equilibrium temperatures. The negative $\Delta^{13}CH_3D$ values are characteristic of kinetic isotope effects during microbial methanogenesis.[5,13,22] The highly negative $\Delta^{12}CH_2D_2$ value for microbial methane is consistent with results of Young et al. (2017)[9] reported for several other methanogenic cultures.

Our results in Figure 5 and Table 2 demonstrate that the measurements of $^{12}CH_2D_2$ can be used to identify methane that carry clumped isotopologue abundances consistent with internal isotopic near-equilibrium (e.g., AL1, AS2 and US-1, SV1, SV2) versus those which carry non-equilibrium abundances (e.g., NS1, NS2 and EM1). Therefore, precise measurements of combined $\Delta^{13}CH_3D$ and $\Delta^{12}CH_2D_2$ values allow us evaluate whether methane was generated via near-equilibrium or kinetic process and if isotopologue thermometry can be used to gauge its temperature of generation.

Table 2. Isotopologue ratios measured with the $^{12}D_2$ – TILDAS. Ratios are expressed as average ± 95% C.I. (NS= Natural sample, SV= Steam vents). T-^{13}D and T-D_2 are estimated temperatures derived from $\Delta^{13}CH_3D$ and $\Delta^{12}CH_2D_2$, respectively.

Sample	$\delta^{13}C$ (‰)	δD (‰)	$\Delta^{13}CH_3D$ (‰)	$\Delta^{12}CH_2D_2$ (‰)	T_{13D} (°C)	T_{12D2} (°C)
Reference and isotopologue spiked methane						
AL1	-34.50 ± 0.02	-147.70 ± 0.06	2.33 ± 0.05	4.4 ± 0.5	214 +25/-22	247 +26/-22
AS2	-38.60 ± 0.05	-153.70 ± 0.30	2.33 ± 0.14	5.7 ± 0.5	214 +17/-15	201 +22/-10
US-1	-38.60 ± 0.23	-153.90 ± 0.18	2.20 ± 0.21	3.3 ± 0.8	228 +24/-21	308 +64/-46
AL1-D3	-35.24 ± 0.06	239.81 ± 0.15	1.49 ± 0.14	26.4 ± 0.6	327 +30/-27	n.a.*
AS1-DY	-44.27 ± 0.06	-403.34 ± 0.43	5.06 ± 0.17	324.3 ± 1.1	50 +7/-7	n.a *
AL1-CD	-82.44 ± 0.72	-158.00 ± 0.18	15.79 ± 0.45	5.5 ± 1.9	n.a.*	205 +12/-11
Natural Samples and cultures						
NS1	-58.12 ± 0.13	-279.16 ± 0.13	1.85 ± 0.18	0.8 ± 0.8	269 +27/-24	623 +406/-164
NS2	-75.93 ± 0.20	-184.96 ± 0.22	4.47 ± 0.28	12.1± 0.8	74 +13/-12	88 +9/-9
EM1	-51.45 ± 0.05	-330.04 ± 0.05	-1.91 ± 0.07	-47.5 ± 0.2	n.a.*	n.a. *
SV1	-22.32 ± 0.24	-127.40 ± 0.15	0.97 ± 0.10	0.2 ± 0.4	447 +26/-23	860 +112/-91
SV2	-23.50 ± 0.22	-126.06 ± 0.17	1.14 ± 0.30	-0.01 ± 0.6	400 +90/-65	>769

*these temperatures are not derived because large positive $\Delta^{13}CH_3D$ (and $\Delta^{12}CH_2D_2$) values for synthetic mixtures are beyond the range of theoretical fit, and negative values do not return apparent equilibrium temperatures.

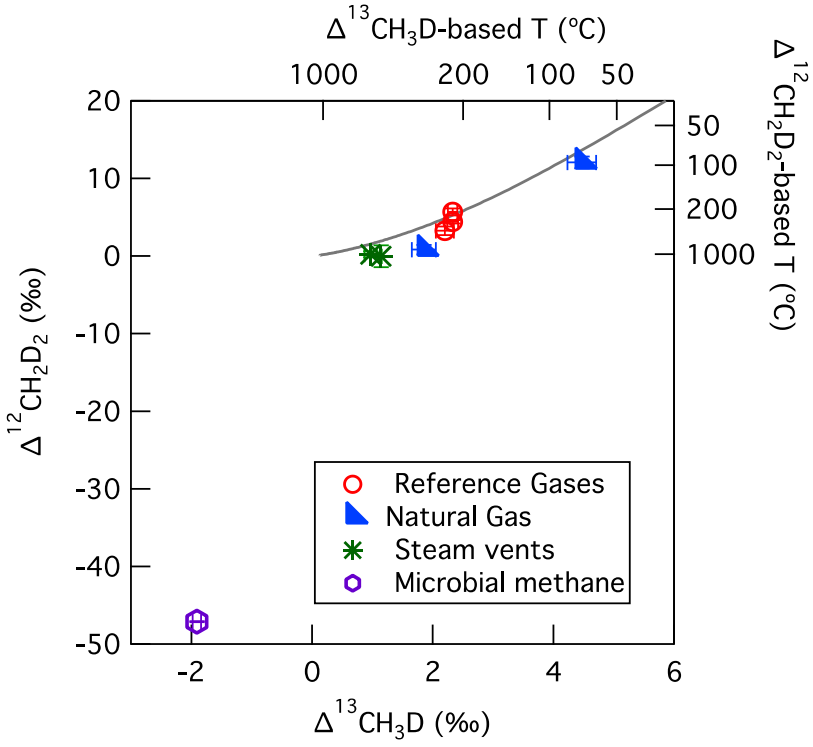

Figure 5. $\Delta^{13}CH_3D$ and $\Delta^{12}CH_2D_2$ for reference gas (AL1, AS2, and US-1) in solid dots, natural gas (NS1, NS2, NS3) in solid triangles, microbial methane (EM1) in open hexagon, and methane from steam vents in open circles. Errors (95% confidence interval) are about the size of the symbols.

CONCLUSIONS

We present the precise measurements of $^{12}CH_2D_2$ abundance of natural isotopologue abundance methane using a tunable infrared laser direct absorption spectroscopy (TILDAS) instrument, equipped with two quantum cascade lasers and a 413m path-length astigmatic multipass absorption cell. The instrument measures ro-vibrational transitions for five isotopologues of methane ($^{12}CH_4$, $^{13}CH_4$, $^{12}CH_3D$, $^{13}CH_3D$, and $^{12}CH_2D_2$) in the 8 and 9 μm regions, corresponding to C-H and C-D bending vibrations. Absorptivity of $^{12}CH_2D_2$ was ca. 0.15% at a cell pressure of 5 Torr (~20 mL STP CH_4), yielding a precision of 0.5‰ over 150 seconds of measurements. We constructed an automated gas injection system that allows injection of reference and sample gas at a constant cell pressure, recovery of sample by cryogenic trapping, and reinjection for repeated measurement cycles. Overall precision for sample versus reference analysis using the sample recycling scheme was ~1‰ for $\delta^{12}CH_2D_2$ and $\Delta^{12}CH_2D_2$, and 0.3‰ for $\Delta^{13}CH_3D$. The latter is of similar precision to our previous instrument using a 76 m pathlength absorption cell with ca. 1 mL STP CH_4. The accuracy of our measurements is limited by non-linearity in the $\delta^{12}CH_2D_2$ scale due to imperfect line profile to describe baseline. This is critical, in particular, for samples with low δD values.

The combined measurements of $\Delta^{13}CH_3D$ and $\Delta^{12}CH_2D_2$ of a set of methane from working reference cylinders, isotopologue spiked, and natural samples highlights the application space of these novel measurements to distinguish between methane carrying isotopologue abundances characterized by near-equilibrium distributions. TILDAS instruments provide an alternative means to high-resolution mass spectrometers, offering the benefits of speed of analysis (several hours instead of a day) and a smaller size and lower cost although TILDAS requires larger sample size than the high-resolution mass spectrometer. Further improvements on the design, such as reducing the cell volume or improving the signal-to-noise ratio would improve the accuracy and reduce the sample size, and thus extend the possibilities of this instrument to measure methane from different sources.

ASSOCIATED CONTENT

Supporting Information

This material is available free of charge via the Internet at http://pubs.acs.org.

- Analysis of the target regions using pure isotopologues
- Effect of trace amount of water on $^{12}CH_2D_2$ measurements
- Abundance sensitivity and the accuracy of $\Delta^{12}CH_2D_2$ measurements
- Sample purification procedures
- Intercomparison of $\Delta^{13}CH_3D$ measured with $^{12}D_2$-TILDAS and our previous ^{13}D-TILDAS
- Supporting Figures and Tables

AUTHOR INFORMATION

Corresponding Author

* E-mail: sono@mit.edu

Notes

The authors declare no competing financial interest.

ACKNOWLEDGMENTS

This project is funded by ExxonMobil Research & Engineering/MIT Membership and Research Agreement for Founding Members, with an Effective Date of September 30, 2014, Agreement #EM09079, Appendix C. This work was supported by ExxonMobil through its membership in the MIT Energy Initiative. The authors thank William Olszewski (MIT), Mike Agnese, Mike Moore and Stanley Huang (Aerodyne), Michael Lawson and Frank Chen (ExxonMobil) for technical assistance. We also like to thank Jeemin H. Rhim and Patrick C. Beaudry for providing methane samples.

REFERENCES

(1) Schaefer, H; Mikaloff Fletcher, S. E.; Veidt, C.; Lassey, K. R., Brailsford, G. W.; Bromley, T. M.; Dlugokencky, E. J.; Michel, S. E.; Miller, J. B.; Levin, I.; Lowe, D. C.; Martin, R. J.; Vaughn, B. H.; White, J. W. C. A 21st-century shift from fossil-fuel to biogenic methane emissions indicated by $^{13}CH_4$, *Science*, **2016**, *352*, 6281, 80-84.

(2) Zou, C; Zhao, Q.; Zhang, G.; Xiong, B.; *Natural Gas Industry B*, **2016**, *3*, 1-11.

(3) Webster, C. R.; Mahaffy, P. R.; Atreya, S. K.; Flesch, G. J.; Farley, K. A.; MSL Science Team, Low Upper Limit to Methane Abundance on Mars, *Science*, **2013**, 342, 355-357

(4) Whiticar, M. J.; Faber, E.; Schoell, M.; Biogenic methane formation in marine and freshwater environments: CO_2 reduction vs acetate fermentation–Isotope evidence, *Geochim. Cosmochim. Acta*, **1986**, *50*, 693–709.

(5) Stolper, D. A.; Sessions, A. L.; Ferreira, A. A.; Santos Neto, E. V.; Schimmelmann, A.; Shusta, S. S.; Valentine, D. L.; Eiler, J. M. Combined 12C-D and D-D clumping in methane: Methods and preliminary results, *Geochimica et Cosmochimica Acta*, **2014**, *126*, 169-191.

(6) Ono, S.; Wang, D. T.; Gruen, D. S.; Sherwood Lollar, B.; Zahniser, M. S.; McManus, B. J.; Nelson, D. D.; Measurement of a doubly substituted methane isotopologue, 13CH3D, by tunable infrared laser direct absorption spectroscopy, *Anal. Chem.*, **2014**, *86*, 6487–6494.

(7) Young, E. D.; Rumble, D.; Freedman, P.; and Mills, M. A large-radius high-mass-resolution multiple-collector isotope ratio mass spectrometer for analysis of rare isotopologues of O_2, N_2, CH_4 and other gases, *International Journal of Mass Spectrometry*, **2016**, *401*, 1–10.

(8) Gunter, B. D.; Musgrave, B. C. New evidence on the origin of methane in hydrothermal gases, *Geochimica et Cosmochimica Acta*, **1971**, *55*, 113-118.

(9) Young, E. D.; Kohl, I. E.; Sherwood Lollar, B.; Etiope, G.; Rumble III, D.; Li, S.; Haghnegahdar, M. A.; Schauble, E. A.; McCain, K. A.; Foustoukos, D. I.; Sutclife, C.; Warr, O.; Ballentine, C. J.; Onstott, T. C.; Hosgormez, H.; Neubeck, A.; Marques, J. M.; Pérez-Rodríguez, I.; Rowe, A. R.; LaRowe, D. E.; Magnabosco, C.; Yeung, L. Y.; Ash, J. L.; Bryndzia, L. T. The relative abundances of resolved $^{12}CH_2D_2$ and $^{13}CH_3D$ and mechanisms controlling isotopic bond ordering in abiotic and biotic methane gases, *Geochimica et Cosmochimica Acta*, **2017**, *203*, 235–264.

(10) Harris, E.; Nelson, D. D.; Olszewski, W.; Zahniser, M.; Potter, K. E.; McManus, B. J.; Whitehill, A.; Prinn, R. G.; Ono, S. Development of a spectroscopic technique for continuous online monitoring of oxygen and site-specific nitrogen isotopic composition of atmospheric nitrous oxide, *Anal. Chem.*, **2014**, *86*, 1726–1734.

(11) Walker, S. A.; Azetsu-Scott, K.; Normandeau, C.; Kelley, D. E.; Friedrich, R.; Newton, R.; Schlosser, P.; McKay, J. L.; Abdi, W.; Kerrigan, E.; Craig, S. E.; Wallace, D. W. R.; Oxygen isotope measurements of seawater ($H_2{}^{18}O/H_2{}^{16}O$): A comparison of cavity ring-down spectroscopy (CRDS) and isotope ratio mass spectrometry (IRMS), *Limnol. Oceanogr.: Methods*, **2016**, *14*, 31–38.

(12) McManus, J. B.; Zahniser, M S.; Nelson, D. D. Dual quantum cascade laser trace gas instrument with astigmatic Herriott cell at high pass number, *Appl. Opt.*, **2011**, *50*, A74-A85.

(13) Wang, D. T.; Gruen, D. S.; Lollar, B. S.; Hinrichs, K.-U.; Stewart, L. C.; Holden, J. F.; Hristov, A. N.; Pohlman, J.W.; Morrill, P. L.; Knneke, M.; Delwiche, K. B.; Reeves, E. P.; Sutcliffe, C.N.; Ritter, D. J.; Seewald, J. S.; Mc Intosh, J. C.; Hemond, H. F.; Kubo, M.D.; Cardace, D.; Hoehler, T. M.; and Ono, S. Nonequilibrium clumped isotope signals in microbial methane, *Science*, **2015**, *348*, 428–431.

(14) Stolper, D. A.; Martini, A. M.; Clog, M.; Douglas, P. M.; Shusta, S. S.; Valentine, D. L.; Sessions, A. L.; Eiler, J. M. Distinguishing and understanding thermogenic and biogenic sources of methane using multiply substituted ispotopologues, *Geochimica et Cosmochimica Acta*, **2015**, *161*, 219-247.

(15) Ma, Q.; Wu, S.; Tang, Y. *Geochim. Cosmochim. Acta*, **2008**, *72*, 5446−5456.

(16) Hut, G. *Consultants' group meeting on stable isotope reference samples for geochemical and hydrological investigations*, *Report to Director General*, IAEA Vienna (Austria) **1987**.

(17) Gordon, I. E.; Rothman, L. S.; Hill, C.; Kochanov, R. V.; Tan, Y.; Bernath, P. F.; Birk, M.; Boudon, V.; Campargue, A.; Chance, K.V.; Drouin, B. J.; Flaud, J.-M.; Gamache, R. R.; Hodges, J. T.; Jacquemart, D.; Perevalov, V.I.; Perrin, A.; Shine, K. P.; Smith, M.-A.H.; Tennyson, J.; Toon, G. C.; Tran, H.; Tyuterev, V. G.; Barbe, A.; Császár, A .G.; Devi, V. M.; Furtenbacher, T.; Harrison, J. J.; Hartmann, J.-M.; Jolly, A.; Johnson, T. J.; Karman, T.; Kleiner, I.; Kyuberis, A. A.; Loos, J.; Lyulin, O. M.; Massie, S. T.; Mikhailenko, S. N.; Moazzen-Ahmadi, N.; Müller, H. S. P.; Naumenko, O. V.; Nikitin, A. V.; Polyansky, O. L.; Rey, M.; Rotger, M.; Sharpe, S. W.; Sung , K.; Starikova, E. ; Tashkun, S. A.; Vander Auwera, J; Wagner, G.; Wilzewski, J.; Wcisło, P.; Yu, S.; Zak, E. J.; *Journal of Quantitative Spectroscopy and Radiative Transfer*, **2017**, *203*, 3-69.

(18) Western, C. M. A Program for Simulating Rotational, Vibrational and Electronic Spectra. *Journal of Quantitative Spectroscopy and Radiative Transfer*, **2016**, *186*, 221-242.

(19) Ulenikov, O. N.; Tolchenov, R. N.; Koivusaari, M.; Alanko, S.; Anttila, R. High Resolution Fourier Transform spectra of CH_2D_2. Pentade of the lowest interacting vibrational bands: $\nu_4(A_1)$, $\nu_7(B_1)$, $\nu_9(B_2)$, $\nu_5(A_2)$ and $\nu_3(A_1)$. *Journal of Molecular Spectroscopy*, **1994**, *167*, 109-130.

(20) Ulenikov, O. N.; Bekhtereva, E. S.; Grebneva, S. V.; Hollensteinb, H.; Quack, M. High resolution Fourier transform spectroscopy of CH_2D_2 in the region 2350–2650 cm^{-1}: the bands $\nu5 + \nu7$, $2\nu9$, $\nu3 + \nu4$, $\nu3 + \nu7$ and $\nu5 + \nu9$, *Phys. Chem. Chem. Phys.*, **2005**, *7*, 1142-1150.

(21) Kosterev, A; Wysocki, G.; Bakhirkin, Y.; So, S.; Lewicki, R.; Fraser, M.; Tittelu, F.; Curl, R. F. Application of quantum cascade lasers to trace gas analysis, *Appl. Phys. B*, **2008**, *90*, 165–176.

(22) Gruen, D. S.; Wang, D. T.; Könneke, M.; Topçuoglu, B. D.; stewart, L. C.; Goldhammer, T.; Holden, J. F.; Hinrichs, K.-U.; Ono, S. Experimental investigation on the controls of clumped isotopologue and hydrogen isotope ratios in microbial methane, *Geochimica et Cosmochimica Acta*, **2018**, *237*, 339-356.

(23) Fiebig, J.; Hofmann, S; Tassi, F.; D'Alessandro, W.; Vaselli, O.; Woodland, A.B.; Isotopic patterns of hydrothermal hydrocarbons emitted from Mediterranean Volcanoes, *Chemical Geology*, **2015**, *396*, 152–163.

(24) Douglas, P. M. J.; Stolper, D. A.; Eiler, J. M.; Sessions, A. L., Lawson, M.; Shuai, Y.; Bishop, A.; Podlaha, O. G.; Ferreira, A. A.; Santos Neto, E. V.; Niemann, M'; Steen, A. S.; Huang, L.; Chimiak L.; Valentine, D. L.; Fiebig, J.; Luhmannm, A. J.; Seyfried Jr., W. E.; Etiope, G., Schoell, M.; Inskeep, W. P.; Moran, J. J.; Kitchen, N. K. Methane clumped isotopes: Progress and potential for a new isotopic tracer, *Organic Geochemistry*, **2017**, *113*, 262–282.